Section 6

PHASE BOUNDARIES FOR C-H-O SYSTEM IN EQUILIBRIUM WITH CARBIDES AND OXIDES OF IRON AND NICKEL

6.1 Introduction

In the catalytic conversion of coal to gaseous and liquid fuels, the formation of carbon and metal compounds, such as metal carbides and oxides, have been observed.[1*] The potential for carbon and metal-compound formation can be evaluated by analyzing thermodynamic equilibria between the gaseous C-H-O system and the various solid phases in co-existence. The carbon (graphite) phase boundaries in equilibrium with the C-H-O gas phase have been examined in some detail,[2,3] but the equilibria involving solid metal carbide and oxide phases have received less attention. The availability of thermodynamic data for the carbides and oxides of iron and nickel allows us to evaluate the gas/solid phase boundaries, thus providing insight into the thermodynamic stability of the metal compounds under catalytic operating conditions.

Thermodynamic calculations have been performed for the gas phase C-H-O compositions in equilibrium with Fe_2C (Hagg carbide), Fe_3C (cementite), Fe_3O_4 (magnetite), and Ni_3C over a range of temperatures and pressures. These data establish the phase boundaries for formation of the metal carbide or oxide phases under conditions of interest to catalytic processes used in Fischer-Tropsch synthesis and methanation.

In the following analysis, we consider CO, CO_2, H_2O, CH_4, and H_2 as the most stable gaseous species in the pressure range from 1 to 33.3 atm (15 to 500 psi) at 500 to 800 K. A more exact calculation would make

*References for Section 6 are listed on page 6.7.

it necessary to include higher molecular weight species containing C, H, and O, but their contribution to the phase-boundary analysis is expected to be small. For our calculations we selected cementite (Fe_3C), Hagg carbide (Fe_2C), nickel carbide (Ni_3C) and iron oxide (Fe_3O_4). In part, we based this choice of solid phases on the availability of thermodynamic data for these compounds and their potential role in catalytic methanation and Fischer-Tropsch synthesis.

6.2 Thermodynamic Considerations

According to the phase rule, complete specification of a system at equilibrium containing five gaseous component (CO, CO_2, H_2O, CH_4, H_2) and two solid-phase components (metal, metal carbide, or oxide) requires a total of six variables. We chose the following variables:

(a) Total gas pressure ($P = p_{CO} + p_{CO_2} + p_{H_2O} + p_{CH_4} + p_{H_2}$)

(b) Temperature

(c) C/H or O/H ratio (gas phase)

and equilibrium constants for three independent reactions. In the case of Fe_3C, we evaluated the equilibrium constants of:

$$CH_4 + 3Fe(\alpha) = Fe_3C(s) + 2H_2 \qquad (6\text{-}1a)$$

$$CO_2 + H_2 = CO + H_2O(g) \qquad (6\text{-}2)$$

$$3H_2 + CO = CH_4 + H_2O(g) \qquad (6\text{-}3)$$

In the case of Fe_2C, we replaced reaction (6-1a) by:

$$CH_4 + 2Fe(\alpha) = Fe_2C(s) + 2H_2 \quad . \qquad (6\text{-}1b)$$

The thermodynamic data were taken from the JANAF Tables and the standard free energies of formation of Fe_3C and Fe_2C from Reference 4. For the

phase boundaries involving Ni_3C, we used the standard free energies of formation of Ni_3C reported by Richardson[5] and the reaction

$$CH_4 + 3Ni(s) \rightarrow Ni_3C(s) + 2H_2 \quad . \qquad (6\text{-}1c)$$

In the calculations pertaining to α-iron and magnetite (Fe_3O_4), we used the following independent reactions:[6]

$$3Fe(\alpha) + 4H_2O = Fe_3O_4(s) + 4H_2 \qquad (6\text{-}4)$$

$$3Fe(\alpha) + 4CO_2 = 4CO + Fe_3O_4 \qquad (6\text{-}5)$$

$$3H_2 + CO = CH_4 + H_2O(g) \qquad (6\text{-}6)$$

The standard free energies of formation of Fe_3O_4 (magnetite) were taken from JANAF Tables. The ideal gas law was used over the entire pressure range. In addition, the calculations were based on isothermal conditions at the gas/solid interphase, in the bulk of the solid, and in the gas phase.

6.3 Numerical Analysis

To calculate the gas/solid equilibria involving the metal carbides and oxide, it is necessary to solve five simultaneous equations. Instead of reducing these equations to one equation, a fifth degree polynomial, we transformed them to two quadratic equations in two unknowns. Newton's method was used to solve this system of equations. Details of the numerical method are appended to this section.

6.4 Results

The results of the thermodynamic calculations for the ternary C-H-O system are most informative when represented in terms of solid-phase deposition boundaries in barycentric coordinates (triangular diagram), and gas phase compositions in equilibrium with the solid phase

at different O/H (or C/H) ratios. For the iron carbides systems, the data in Figure 6-1 depict the boundary lines above which Fe_3C or Fe_2C are thermodynamically stable and below which they are absent at equilibrium. Although the phase boundaries for Fe_3C and Fe_2C nearly coincide at 500 K, they begin to separate with increasing temperature (Figures 6-2 to 6-4), with the Fe_2C curve lying above Fe_3C. Of interest is the location of the carbon (graphite)* deposition boundary[2] relative to that of the iron carbides. In the temperature range examined in this study, the carbon boundary is displaced from the Fe_2C and Fe_3C curves in a downward direction (Figures 6-1 and 6-3), indicating the higher stability of C(gr). The phase boundaries calculated for the Ni_3C system at 500 and 700 K are shown in Figures 6-5 and 6-6. Also included are the C(gr) phase boundaries.[3]

The effect of total gas pressure on the phase boundaries of Fe_2C and Fe_3C was evaluated in the range from 1 to 33-1/3 atm. Within the limits of accuracy of the computed data, we detected no change in the phase boundary limits.

For the C-H-O/Fe_3O_4 system, iron oxide exhibits stability in the region below the curve (labeled Fe_3O_4 in Figures 6-1 to 6-4). It is apparent from these calculations that the Fe_3O_4 phase can coexist with Fe_3C and Fe_2C at the points of intersection of the respective boundary curves in the triangular diagrams.

In equilibrium with the different solid phases, the gas phase compositions, in terms of the five stable chemical species under consideration, have been calculated for a range of O/H ratios, indicative for example, of different H_2/CO or H_2O/CO feed ratios. Representative curves at 1 and 33-1/3 atm are shown in Figures 6-7 and 6-8 for equilibria

*Carbon (graphite) is abbreviated as C(gr) throughout this report.

involving Fe_3C and in Figures 6-9 and 6-10 for Fe_2C. At low O/H ratios, methane is the predominant product, but with increasing O/H ratio, oxidation of CH_4, H_2, and CO leads to water and carbon dioxide as the major products. The mole fraction of water goes through a maximum at the stoichiometric ratio O/H = 0.5. At higher O/H the marked increase in CO partial pressure is caused by reaction of the iron carbide with H_2O and by oxidation of methane to CO and CO_2. With increasing pressure the mole fractions CH_4, H_2O, and CO_2 increase, while those of H_2 and CO diminish. A rise in temperature lowers the mole fractions of CH_4 and CO_2 in equilibrium with Fe_3C and Fe_2C but raises those of H_2, CO, and H_2O. These trends can be seen by comparing the curves in Figures 6-7 and 6-11 for Fe_3C, and Figures 6-9 and 6-12 for Fe_2C. Similar considerations apply to the equilibrium product distribution in the presence of Ni_3C (Figures 6-13 and 6-14). In the case of Fe_3O_4 (Figure 6-15) the product distribution is plotted as a function of C/H ratio (rather than O/H). In this presentation, the CH_4 mole fraction reaches a maximum at C/H = 0.25.

6.5 Discussion

In the design and operation of catalytic reactors for methanation, water-gas shift, and Fischer-Tropsch synthesis, the equilibrium boundaries for formation of different solid phases as a function of gas phase composition are important for adjustment of feed-gas composition. For example, the change in gas composition from feed gas to equilibrium is demonstrated by the dashed line for an initial feed ratio $H_2/CO = 3$ at 700 K and 1 atm (Figure 6-3). In following this line in an upward direction toward the C-apex of the triangular diagram, we cross four phase boundaries. The first relates to the C(gr) equilibrium; the second, to the Fe_3C equilibrium; the third, to the Fe_2C equilibrium; and the fourth, to the Fe_3O_4 equilibrium. The gas phase composition, in

equilibrium with Fe_3C, Fe_2C, and Fe_3O_4, for $H_2/CO = 3$ (equivalent to $O/H = 0.167$), can be found from the curves shown in Figures 6-7, 6-9, and 6-15; the gas composition in equilibrium with C(gr) from Reference 2.

For industrial methanation with Ni as a catalyst, the H_2/CO feed gas composition chosen[7] for a number of process designs is $3.24 < H_2/CO < 3.96$. This gas composition is considered to be well outside the carbon- or Ni_3C-forming regions because of rate-limited displacement from equilibrium. However, the presence of hydrocarbon impurities in the feed gas could shift the system across the phase boundary for carbon formation. In Fischer-Tropsch synthesis, the formation of the iron carbides [Fe_2C (Hagg carbide) and Fe_3C (cementite)] has been well documented.[8] Their presence appears to be concomitant to the pretreatment process to which Fe catalysts are subjected in the early stages of Fischer-Tropsch synthesis. Similarly, the presence of Fe_3O_4 as a stable phase has been observed in samples of Fischer-Tropsch catalyst removed from a reactor after several days exposure to syn gas at 10 to 20 atm and 600 to 675 K, including fused-iron and Raney-iron catalysts.[9] Thermomagnetic studies indicated that Fe_2C (Hagg carbide) as well as Fe_3O_4 are present in Raney iron catalysts, whereas the fused-iron catalysts exhibited Fe_3O_4 as the predominant phase.

For the water-gas shift reaction, the phase boundary calculations for the iron system indicate that at typical operating temperatures of 700 to 800 K and $H_2O/CO \geq 1$, the formation of Fe_3O_4 is favored thermodynamically.

Laboratory experiments[9] with fused iron catalysts demonstrate the gradual disappearance of Fe_3C (cementite) and growth of Fe_2C (Hagg carbide) accompanied by carbon deposition when the catalyst is exposed to feed gas at 1 atm ($H_2/CO = 3/1$) and 598 K. We appear to be dealing with kinetically limited transformations to the equilibrium products.

It has generally been assumed[10] that Fe_3C is the result of the reaction $Fe_2C + Fe \rightleftharpoons Fe_3C$. According to the thermodynamic analysis, the reverse process would be more favorable, as confirmed experimentally in our studies (Section 5).

The catalytic properties of the various solid phases are also of interest. In the Ni catalyzed methanation reaction, the bulk Ni_3C phase, although thermodynamically stable, does not form, i.e., the reaction must occur far removed from the equilibrium involving Ni_3C. In Fischer-Tropsch synthesis with Fe catalysts, the carbide phases appear to be important in the synthesis of high molecular weight hydrocarbons. Equilibrium calculations[11] indicate that Fe_2C, CO, and H_2 participation in hydrocarbon synthesis is thermodynamically possible. The same calculations would apply to Fe_3C, because its free energy of formation is nearly the same as that of Fe_2C. It is well known that during carburization of the catalyst, the formation of CH_4 as the major product precedes Fischer Tropsch synthesis of higher molecular weight hydrocarbon. Thus, the iron carbide phase appears to be a key component in the reaction.

The gradual formation of Fe_3O_4, as favored thermodynamically, may lead to deactivation of Fischer-Tropsch catalysts. The Fe-based catalysts are generally in the form of an oxide or a surface-oxidized solid as a starting material. Their catalytic properties for Fischer Tropsch synthesis are acquired by careful reduction and carburization. Ultimately, however, the reaction conditions lead to Fe_3O_4 formation and catalyst decay, indicative of transient catalytic properties favorable for hydrocarbon synthesis.

6.6 References and Notes

1. H. Pichler and H. Schulz, Chemie Ing. Technik, 42, 1162 (1972).

2. E. J. Cairns and A. D. Tevebaugh, J. Chem. Eng. Data, 9, 453 (1964).

3. M. J. Whalen, "Carbon Formation in Methanators," ERDA Report Fe 2240-10, July 1976.

4. J. Chipman, Met. Trans. 3, 55 (1972).

5. F. D. Richardson, J. Iron Steel Inst. 173, 3 (1953).

6. While this work was in progress, the work of M. P. Manning [Thesis, MIT (1976)] on the C-H-O/Fe_3O_4 system, came to our attention. His results are in good agreement with our calculations.

7. M. J. Whalen, Report FE-2240-10, Energy Research and Development Administration, July 1976.

8. H. H. Storch, N. Golumbric, and R. B. Anderson, The Fischer-Tropsch and Related Syntheses, (John Wiley and Sons, New York, 1951).

9. SRI Quarterly Progress Report PERC-0060-6, February 1, 1977, prepared for ERDA under Contract E-(3602)-0060.

10. H. Pichler and H. Schulz, Chemie Ingenieur Technik, 42, 1162 (1972).

11. S. C. Schuman, J. Chem. Phys., 16, 1175 (1948).

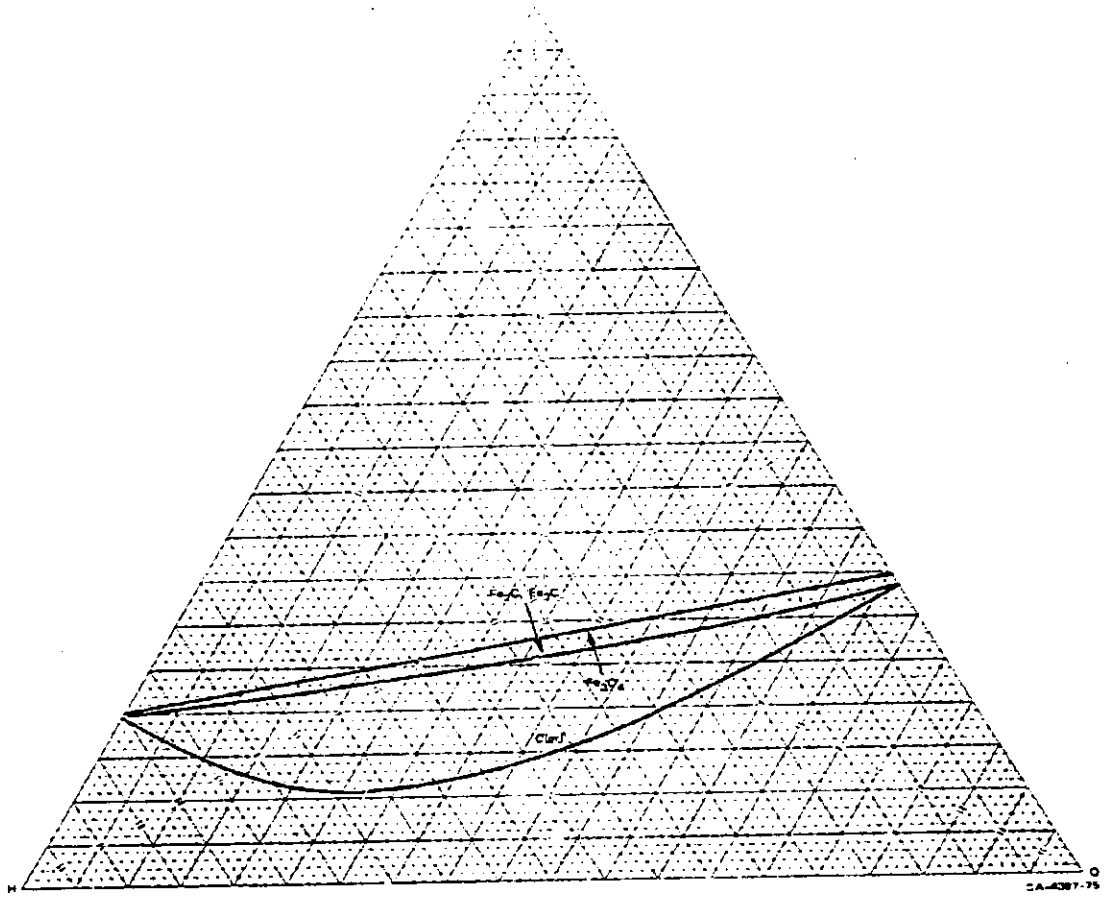

FIGURE 6-1 PHASE BOUNDARIES FOR GASEOUS C,H,O SYSTEM IN EQUILIBRIUM WITH SOLID Fe_3C OR Fe_2C OR Fe_3O_4 AT 500 K AND 1 atm

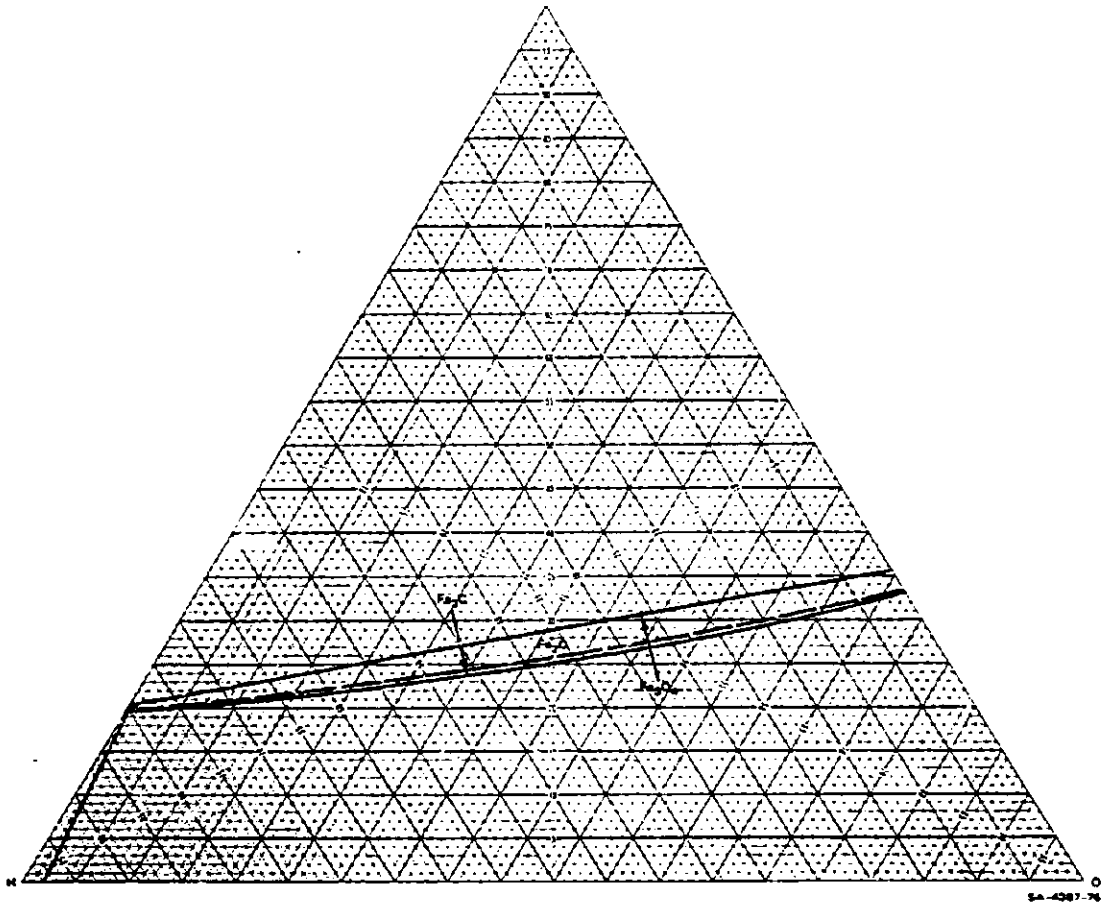

FIGURE 6-2 PHASE BOUNDARIES FOR GASEOUS C,H,O SYSTEM IN EQUILIBRIUM WITH SOLID Fe_3C OR Fe_7C OR Fe_3O_4 AT 600 K AND 1 atm

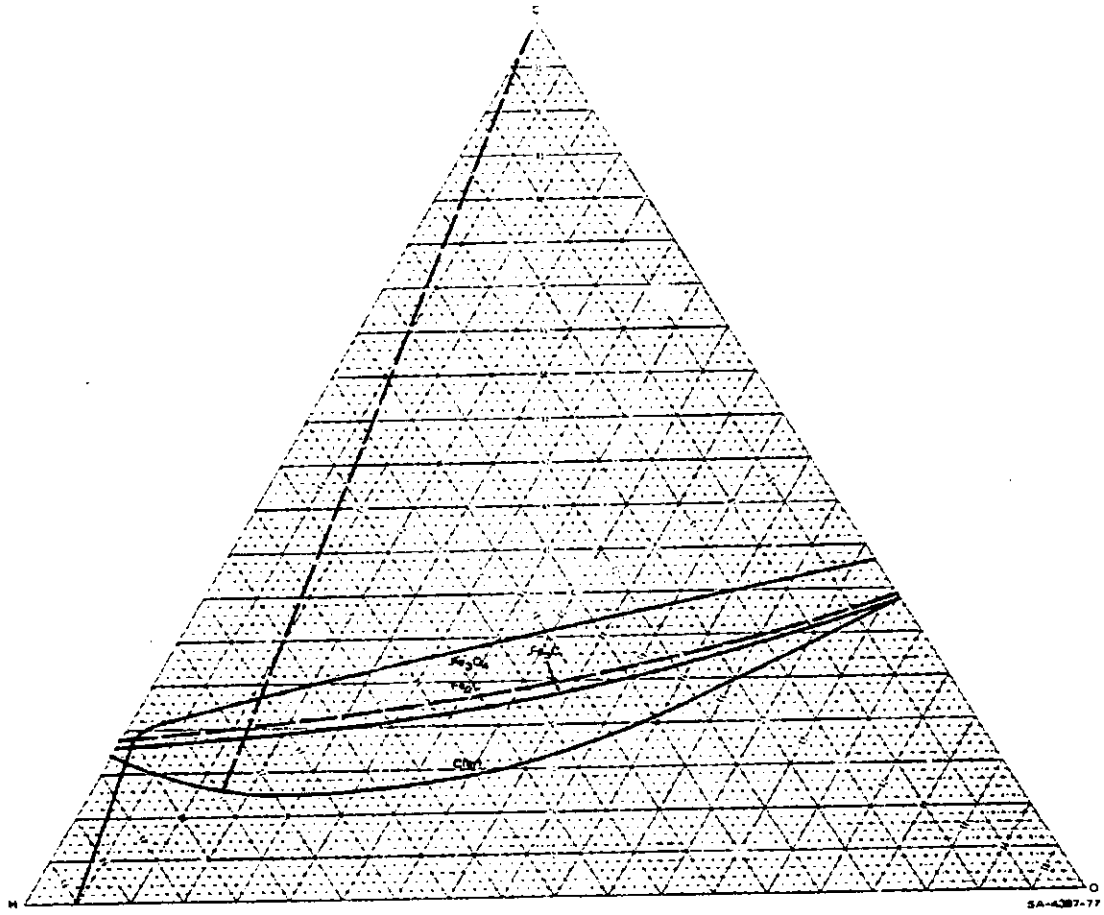

FIGURE 6-3 PHASE BOUNDARIES FOR GASEOUS C,H,O SYSTEM IN EQUILIBRIUM WITH SOLID Fe_3C OR Fe_2C OR C, Fe_3O_4 AT 700 K AND 1 atm

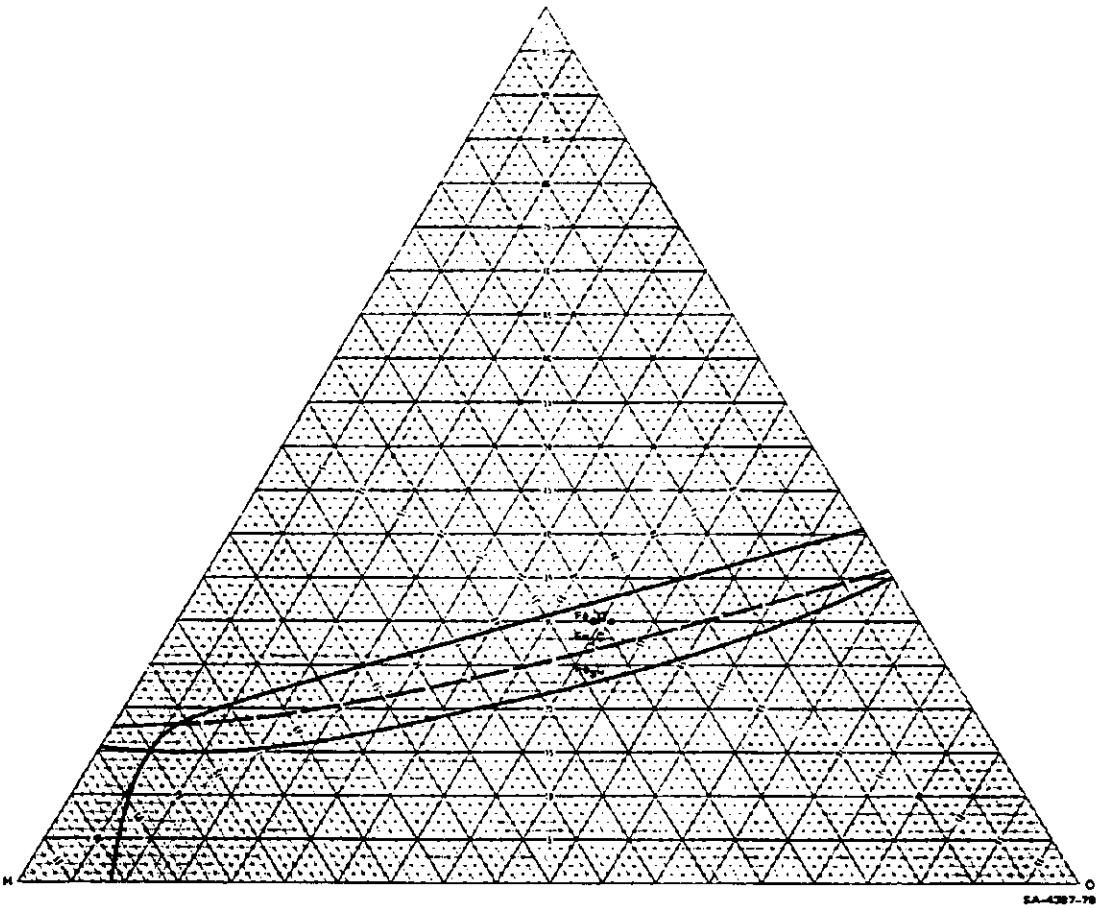

FIGURE 6-4 PHASE BOUNDARIES FOR GASEOUS C,H,O SYSTEM IN EQUILIBRIUM WITH SOLID Fe_3C OR Fe_2C OR Fe_3O_4 AT 800 K AND 1 atm

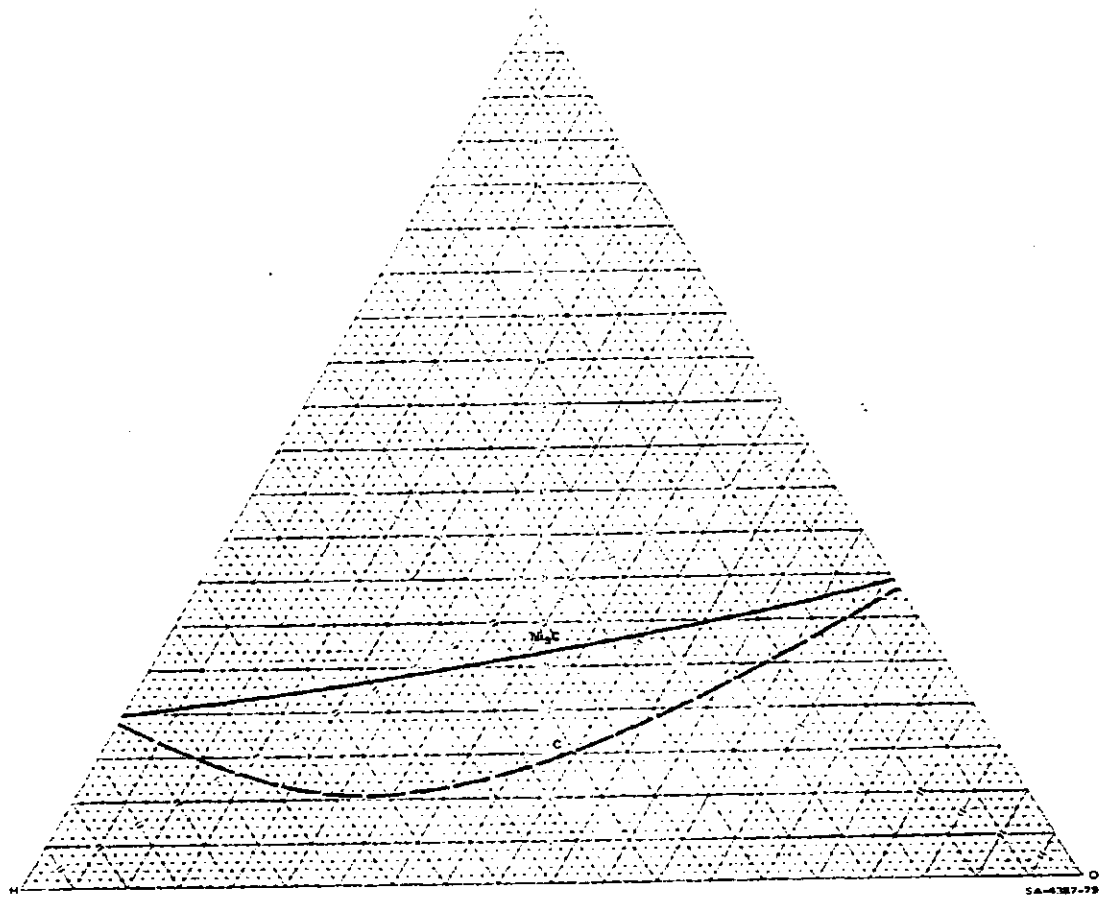

FIGURE 6-5 PHASE BOUNDARIES FOR GASEOUS C,H,O SYSTEM IN EQUILIBRIUM WITH SOLID C OR Ni_3C AT 500 K AND 1 atm

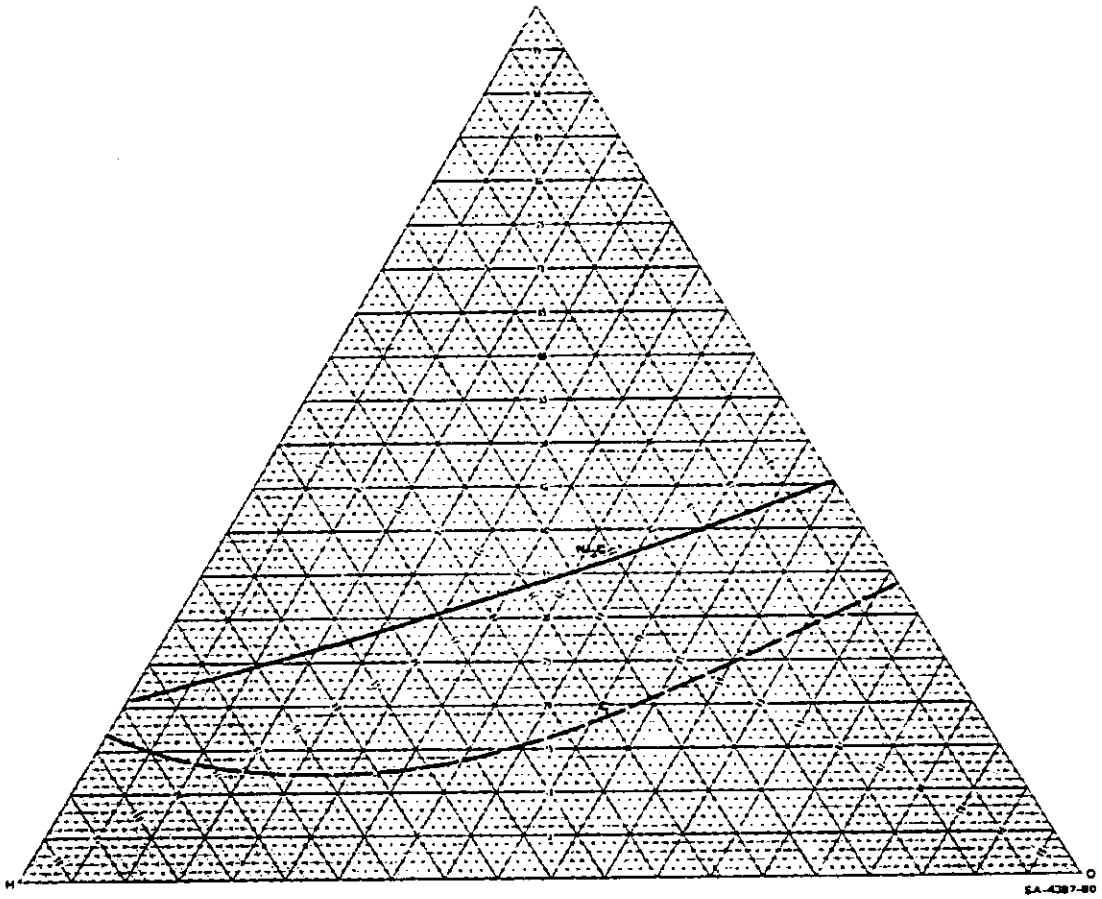

FIGURE 6-6 PHASE BOUNDARIES FOR GASEOUS C,H,O SYSTEM IN EQUILIBRIUM WITH SOLID C OR Ni_3C AT 700 K AND 1 atm

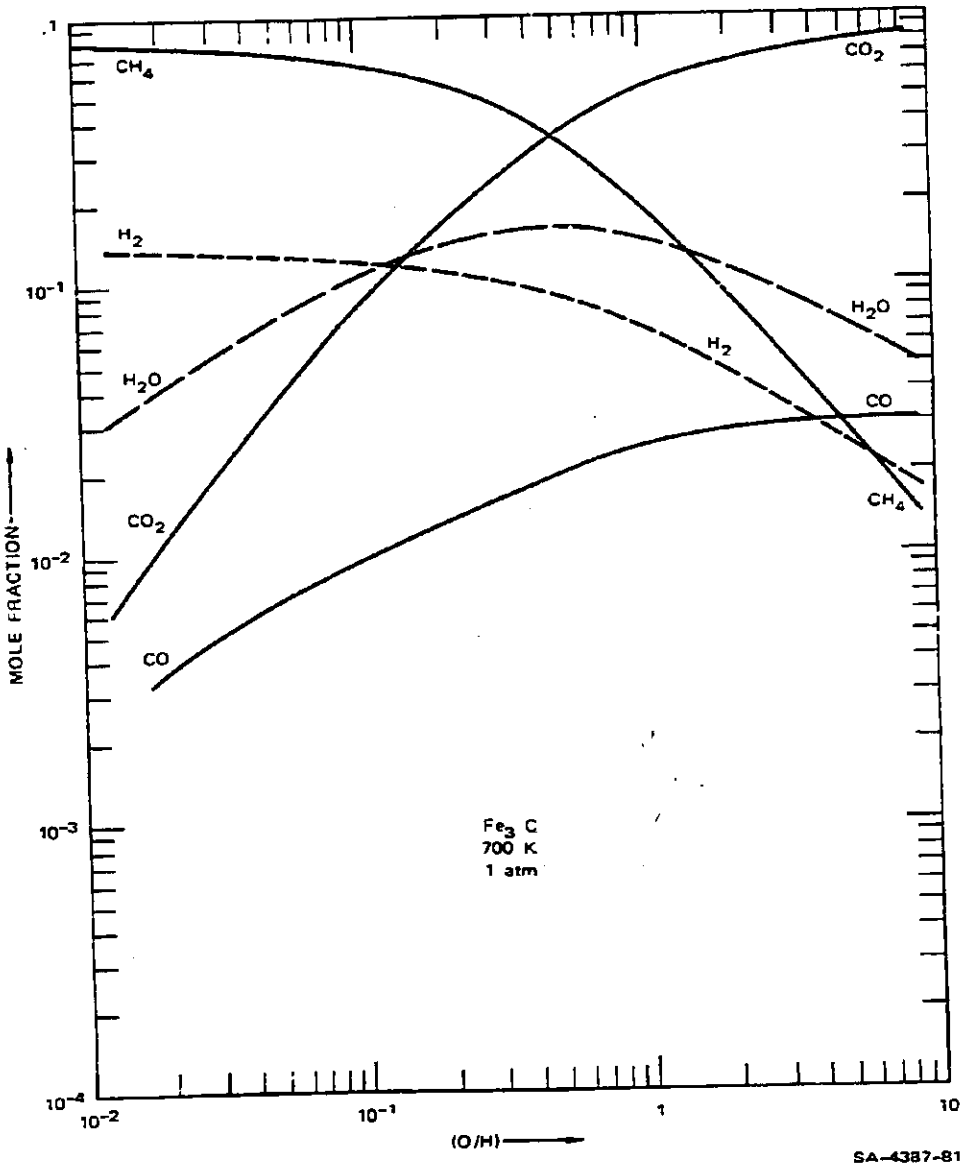

FIGURE 6-7 MOLE FRACTION OF STABLE PRODUCTS IN EQUILIBRIUM WITH Fe_3C AT 700 K AND 1 atm

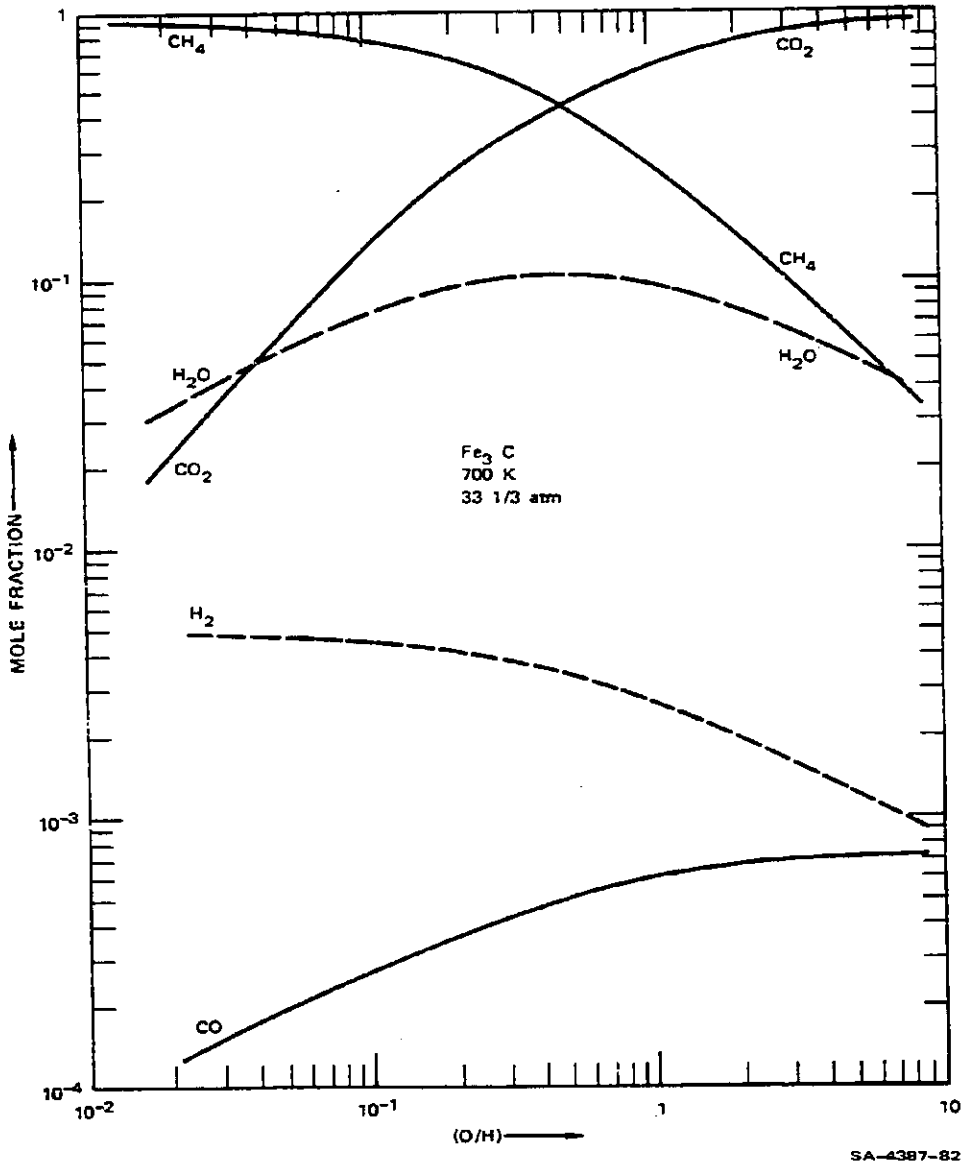

FIGURE 6-8 MOLE FRACTION OF STABLE PRODUCTS IN EQUILIBRIUM WITH Fe_3C AT 700 K AND 33-1/3 atm

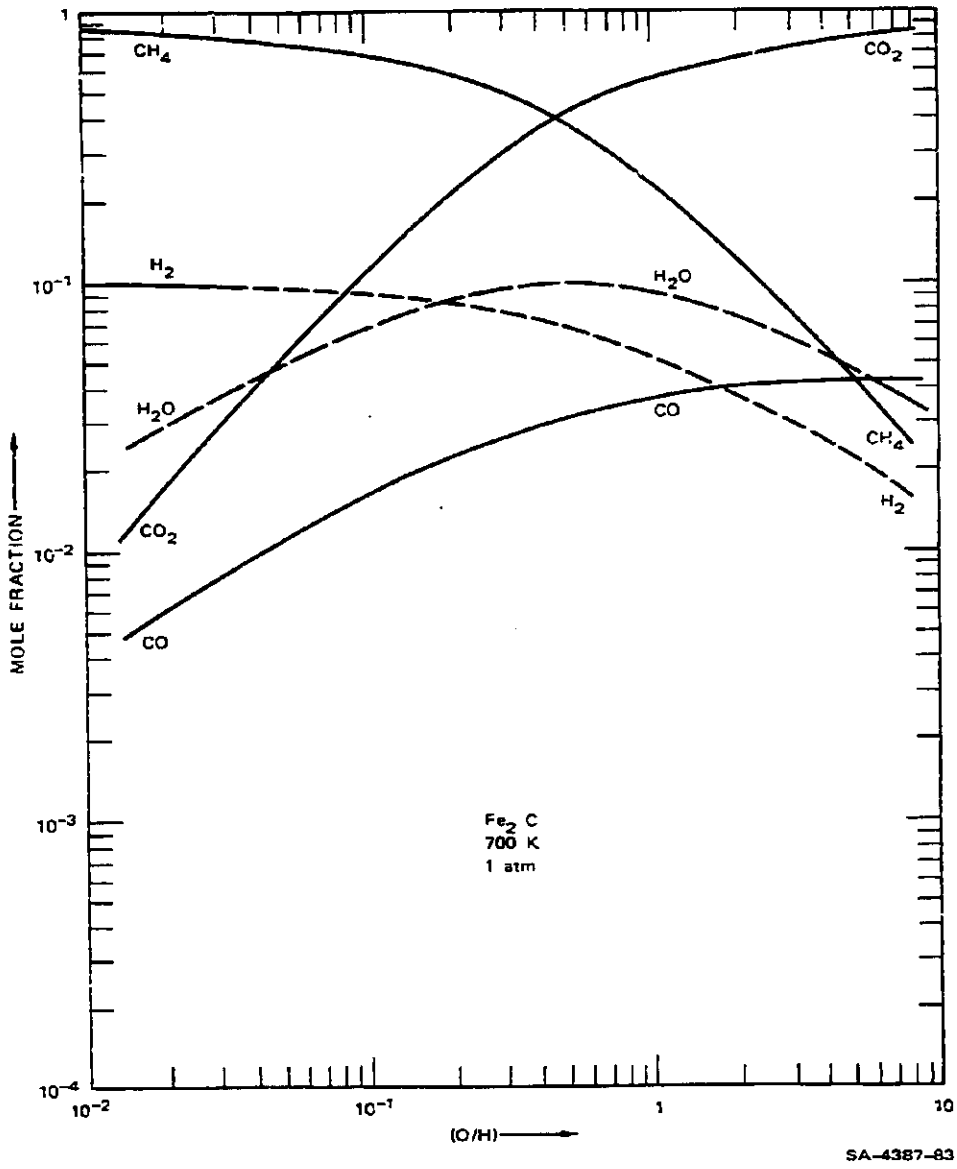

FIGURE 6-9 MOLE FRACTION OF STABLE PRODUCTS IN EQUILIBRIUM WITH Fe_3C AT 700 K AND 1 atm

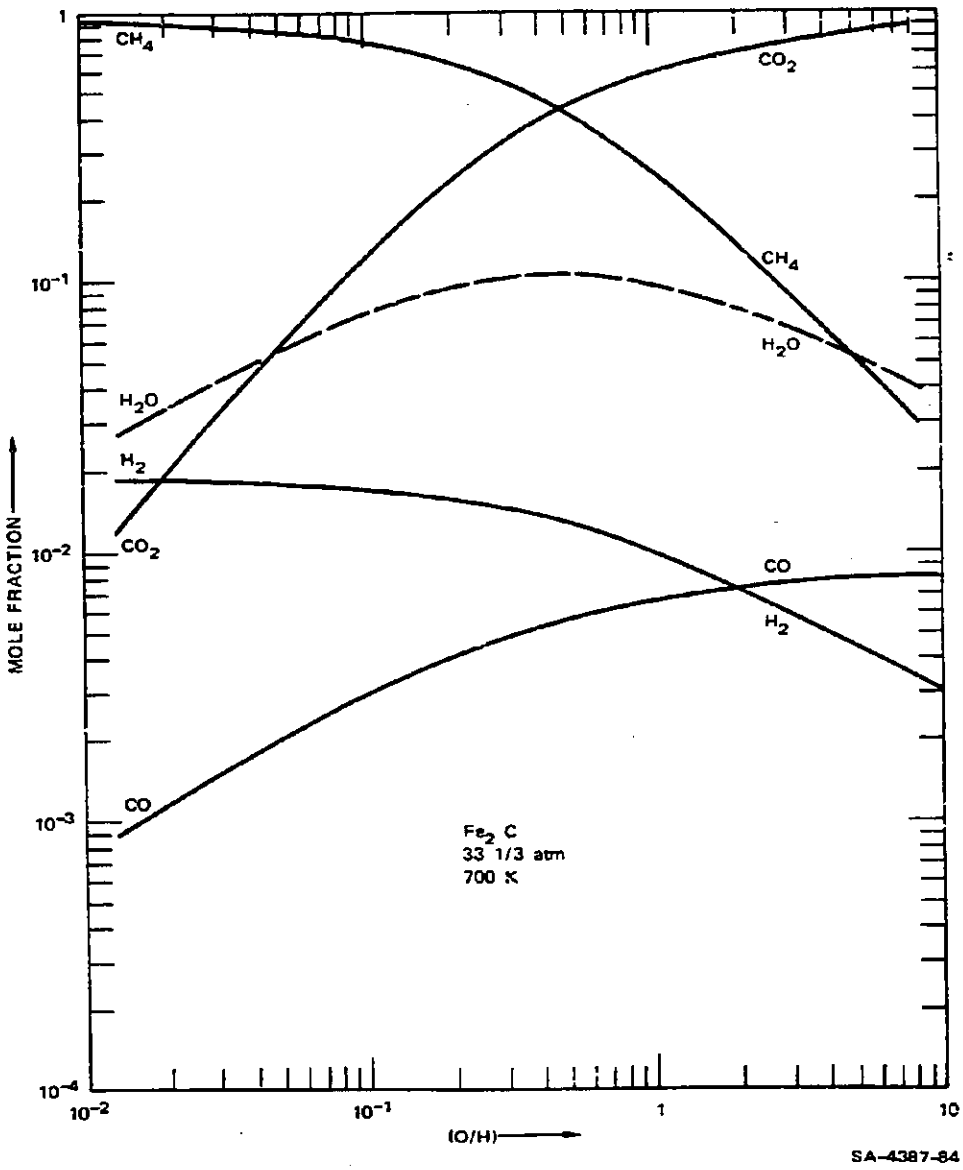

FIGURE 6-10 MOLE FRACTION OF STABLE PRODUCTS IN EQUILIBRIUM WITH Fe_2C AT 700 K AND 33-1/3 atm

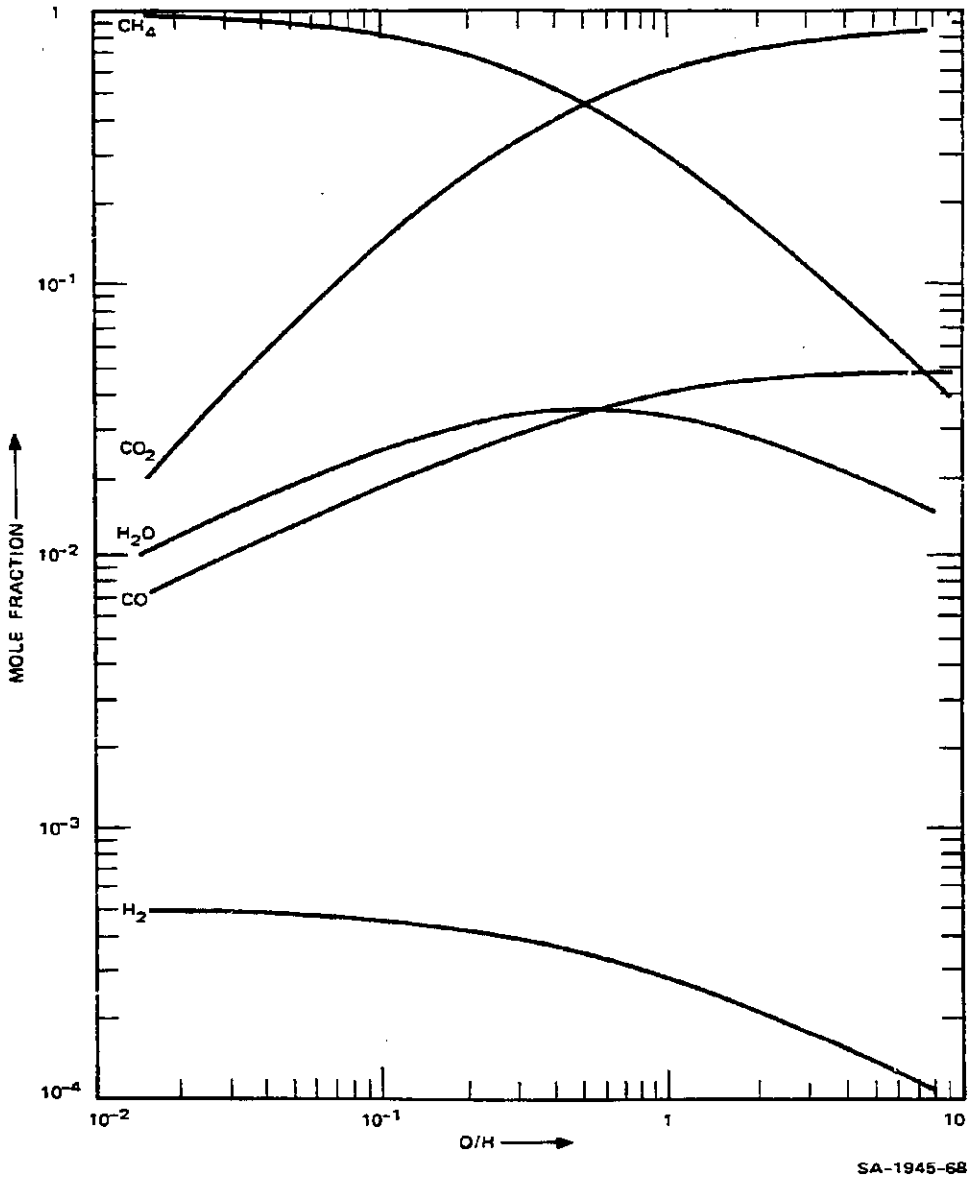

FIGURE 6-11 MOLE FRACTION OF STABLE PRODUCTS IN EQUILIBRIUM WITH Ni_3C AT 500 K AND 1 atm

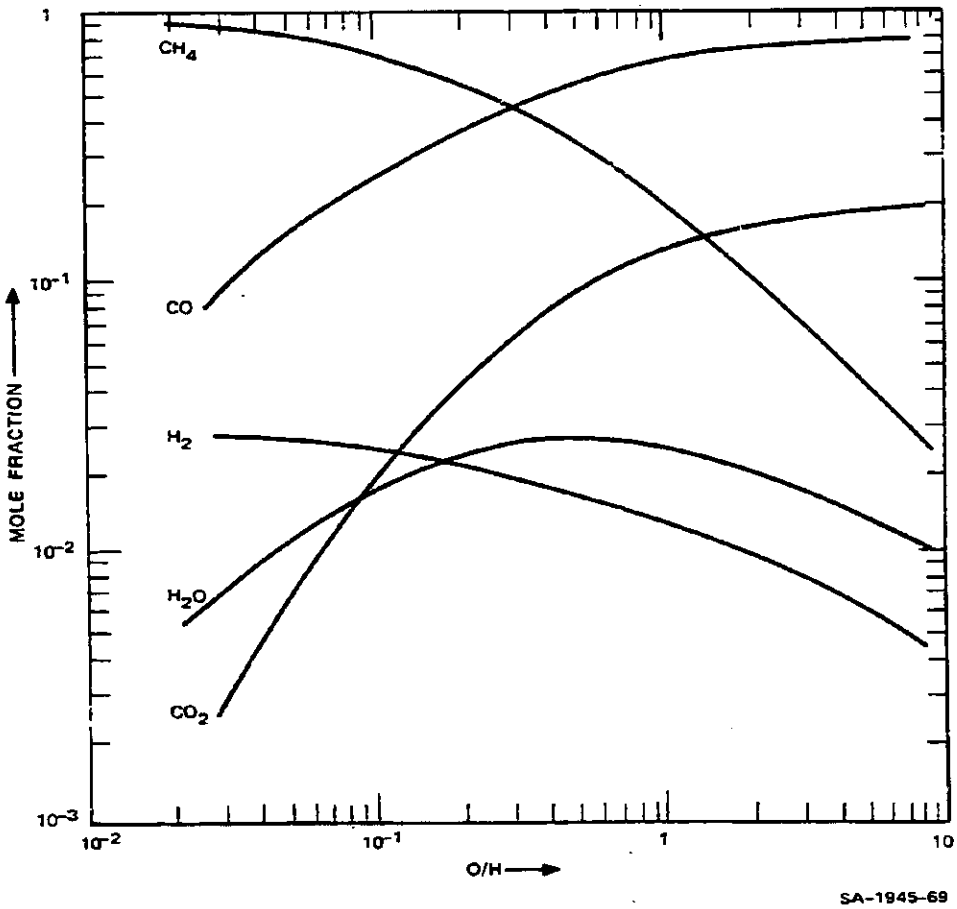

FIGURE 6-12 MOLE FRACTION OF STABLE PRODUCTS IN EQUILIBRIUM WITH Ni_3C AT 700 K AND 1 atm

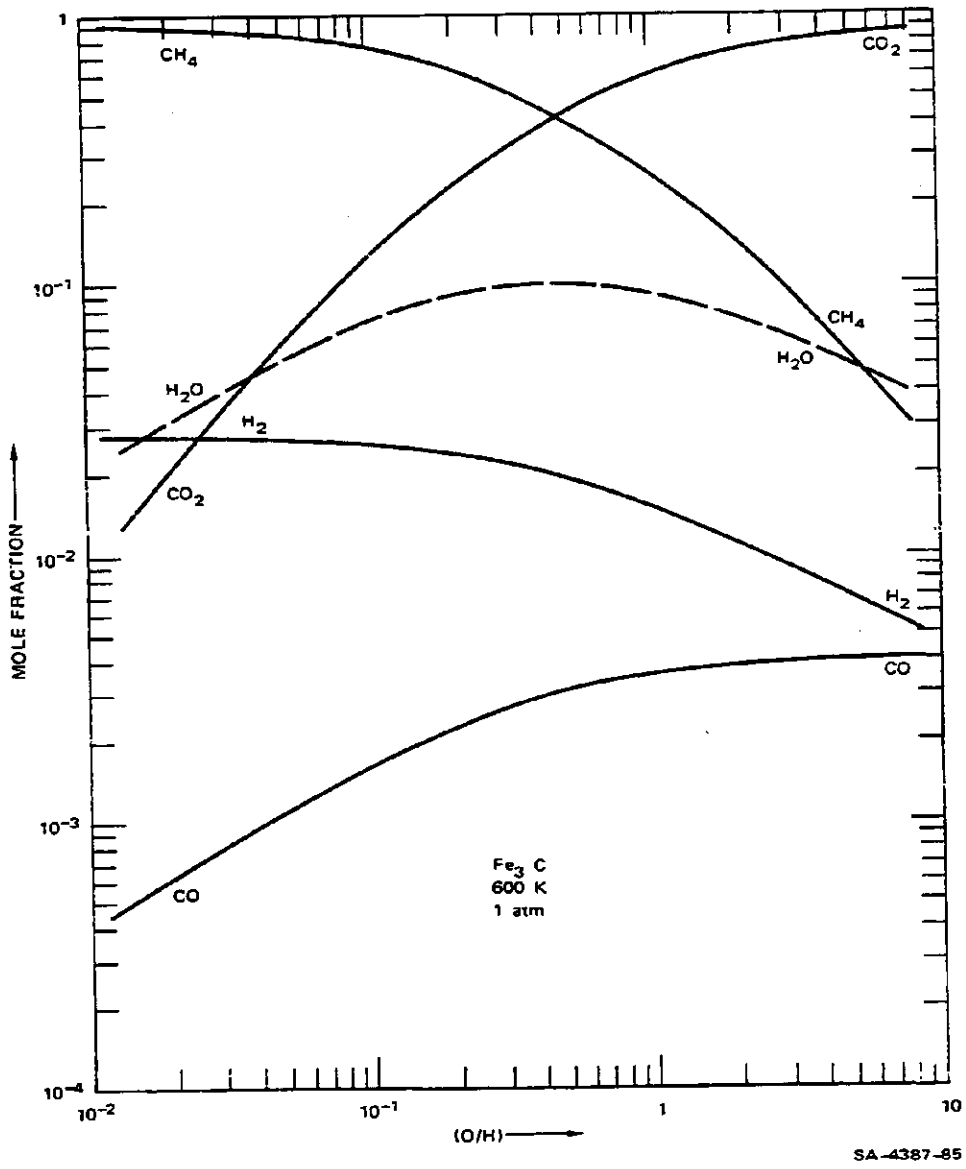

FIGURE 6-13 MOLE FRACTION OF STABLE PRODUCTS IN EQUILIBRIUM WITH Fe_3C AT 600 K AND 1 atm

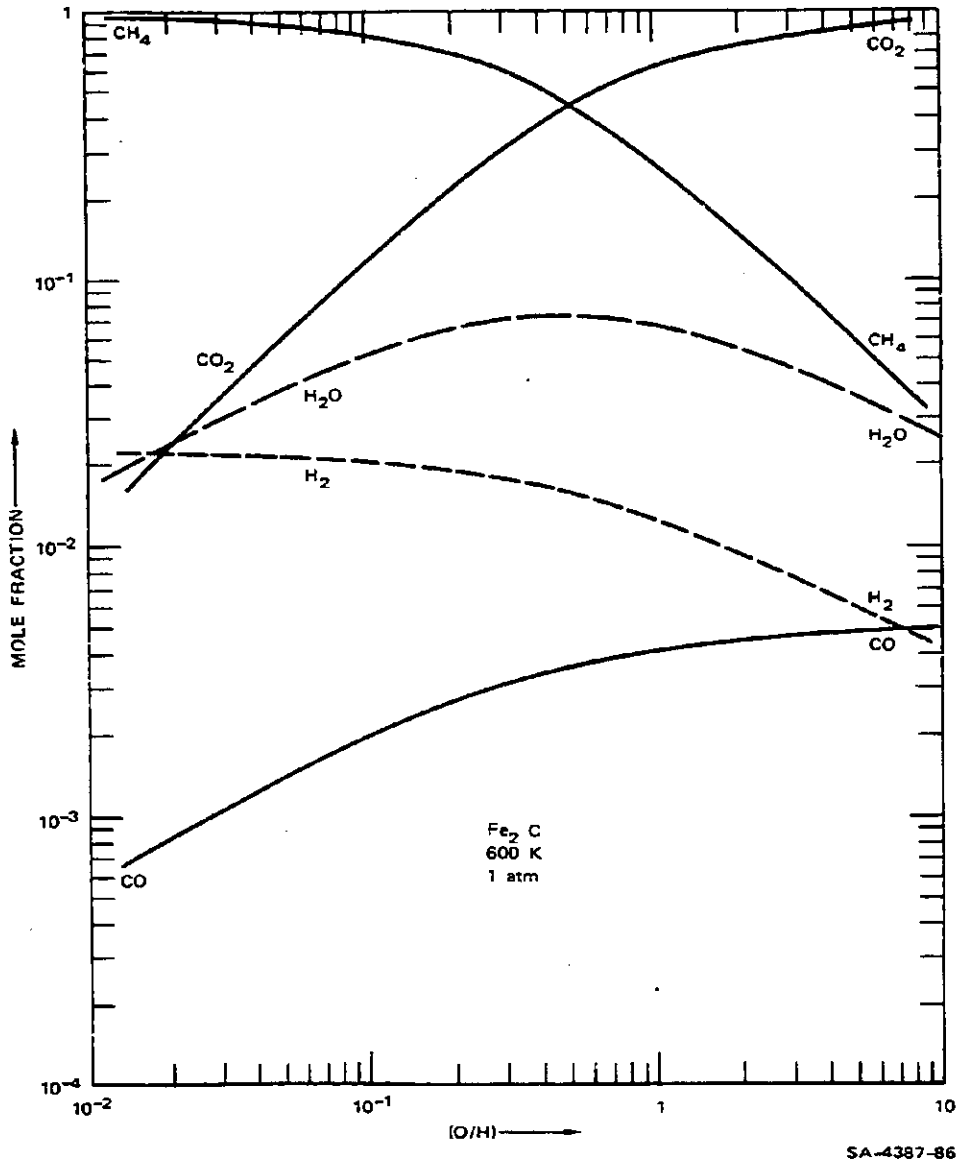

FIGURE 6-14 MOLE FRACTION OF STABLE PRODUCTS IN EQUILIBRIUM WITH Fe_2C AT 600 K AND 1 atm

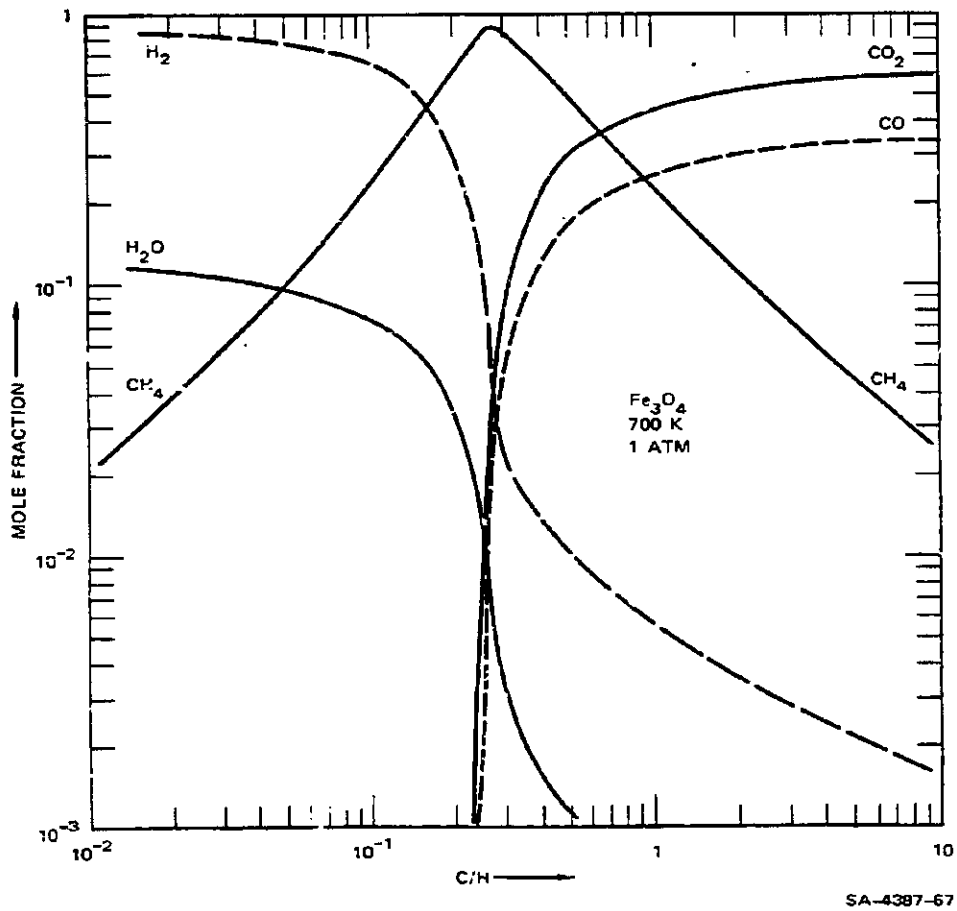

FIGURE 6–15 MOLE FRACTION OF STABLE PRODUCTS IN EQUILIBRIUM WITH Fe_3O_4 AT 700 K AND 1 atm

Appendix to Section 6

DETAILS OF NUMERICAL ANALYSIS

The equilibrium calculations involving the iron carbides require the solution for the five unknowns

$$x_1 = p_{H_2},\ x_2 = p_{CO},\ x_3 = p_{CH_4},\ x_4 = p_{CO_2},\ x_5 = p_{H_2O}$$

of five simultaneous equations:

$$P = x_1 + x_2 + x_3 + x_4 + x_5$$

$$K_1 = x_3/x_1^2 \equiv p_{CH_4}/p_{H_2}^2$$

$$K_2 = (x_2 x_5)/(x_1 x_4) \equiv (p_{CO}\ p_{H_2O})/(p_{H_2}\ p_{CO_2})$$

$$K_3 = (x_3 x_5)/(x_2 x_1^3) \equiv (p_{CH_4}\ p_{H_2O})/(p_{CO}\ p_{H_2}^3)$$

$$\rho = \left(\frac{O}{H}\right)_{gas} = (x_2 + 2\,x_4 + x_5)/(2\,x_1 + 4\,x_3 + 2\,x_5)$$

$$\equiv (p_{CO} + 2\,p_{CO_2} + p_{H_2O})/(2\,p_{H_2} + 4\,p_{CH_4} + 2\,p_{H_2O})\ .$$

Let the temperature be fixed and the three equilibrium constants K_1, K_2, K_3 be given as well as the pressure P and (O/H) ratio ρ.

It is customary to reduce these equations to one equation, a fifth degree polynomial, in x_1. This polynomial is solved for a suitable root, which in turn is used to obtain the other variables.

We will not follow this procedure to completion since for large values of the K_i the coefficients in the polynomial may become quite large, whereas the root sought may be small. This condition could cause numerical instability.

If we eliminate x_3 by

$$x_3 = K_1 x_1^2$$

then

$$x_5 K_1 x_1^2 = K_3 x_2 x_1^3 \quad .$$

If $x_1 \neq 0$, then

$$x_5 \equiv K x_1 x_2$$

where we set $$K = K_3/K_1 \quad .$$

Similarly

$$x_4 = \frac{K}{K_2} x_2^2 \quad .$$

Insertion in the first and last of the original equations yields two quadratic equations in two unknowns:

$$f_1(x_1, x_2) \equiv x_1 + x_2 + x_1(K_1 x_1 + K x_2) + \frac{K}{K_2} x_2^2 - p = 0$$

$$f_2(x_1, x_2) \equiv 2 p x_1(1 + K x_2 + 2 K_1 x_1) - x_2(1 + 2\frac{K}{K_2} x_2 + K x_1) = 0 \quad .$$

To solve this system we use Newton's method for the above system:

$$\begin{pmatrix} a & b \\ c & d \end{pmatrix}\begin{pmatrix} d_1 \\ d_2 \end{pmatrix} = \begin{pmatrix} a\ d_1 + b\ d_2 \\ c\ d_1 + d\ d_2 \end{pmatrix} = -\begin{pmatrix} f_1^o \\ f_2^o \end{pmatrix} \qquad (6\text{-}7)$$

where (x_1^o, x_2^o) is a guessed point, $f_i^o = f_i(x_1^o, x_2^o)$, and the corrected point $(x_1, x_2)^1$ is given by:

$$\begin{pmatrix} x_1^1 \\ x_2^1 \end{pmatrix} = \begin{pmatrix} x_1^o \\ x_2^o \end{pmatrix} + \begin{pmatrix} d_1 \\ d_2 \end{pmatrix} .$$

Thus we must solve the equation (6-7) for d_1 and d_2 where the matrix $\begin{pmatrix} a & b \\ c & d \end{pmatrix}$, the Jacobian of the transformation $\begin{pmatrix} f_1 \\ f_2 \end{pmatrix}$, is evaluated at (x_1^o, x_1^o). That is, $a = f_{11}$, $b = f_{12}$ $c = f_{21}$, and $d = f_{22}$, where f_{ij} is the partial derivative of f_i with respect to x_j. In this case

$$a = 1 + 2\,K_1\,x_1 + K\,x_2$$

$$b = 1 + K\,x_1 + \frac{2K}{K_2}\,x_2$$

$$c = 2\rho(1 + 4\,K_1\,x_1) + K\,(2\rho - 1)\,x_2$$

$$d = -1 + K(2\rho - 1)\,x_1 - 4\,\frac{K}{K_2}\,x_2 \quad .$$

In practice about five iterations are required to get four-place accuracy. Use of the polynomial method is more cumbersome.

For the system involving Fe_3O_4 (magnetite) one has:

$$K_4 = x_1/x_5$$

$$K_5 = x_2/x_4$$

$$K_6 = x_3\, x_5/(x_2\, x_1)^3$$

$$P = \Sigma_1^5\, x_i$$

$$\rho = (x_2 + x_4 + x_3)/(2(x_1 + 2\, x_3 + x_5) \equiv (C/H)_{gas} \quad .$$

Eliminating all but x_1 and x_2 yields

$$P = K_{41}\, x_1 + K_{51}\, x_2 + e\, x_2\, x_1^2$$

$$2\rho = [(K_{51} + e\, x_1^2)\, x_2]/[(K_{41} + 2\, e\, x_1\, x_2)\, x_1]$$

where $K_{41} = 1 + 1/K_4$, $K_{51} = 1 + 1/K_5$, $e = K_4 K_5$.

The two equations may further be written as

$$f_1 \equiv K\, x_1 + \bar{x}\, x_2 - P = 0$$

$$f_2 \equiv 2\rho\bar{y}\, x_1 - \bar{x}\, x_2 = 0$$

where

$$\bar{x} = K_{51} + e\, x_1^2$$

$$\bar{y} = K_{41} + 2e\, x_1 x_2$$

$$K = K_{41} \quad .$$

This system is not quadratic, and the large value of e ($\sim 10^{17}$) makes the use of Newton's method unsatisfactory.

We may further eliminate x_2 from $x_2 = (P - K x_1)/\bar{x}$ so that f_2 becomes

$$f_2 \equiv 2\rho \bar{y} x_1 - (P - K x_1) = 0$$

and inserting the value for $\bar{y}$ yields

$$(2\rho + 1) K x_1 - P + 4\rho \frac{\xi x_1^2}{\bar{x}} (P - K x_1) = 0 \quad .$$

Setting $\tau = e x_1^2/\bar{x}$ we get that

$$(P - K \bar{\rho} x_1)/(P - K x_1) = 4 \rho \tau \qquad (6\text{-}8)$$

where $\bar{\rho} = 2\rho + 1$.

Note that $\tau = (e x_1^2)/(K_{51} + e x_1^2) < 1$

and that for $e x_1^2 \gg K_{51}$, τ is close to 1. Since $\tau(0) = 0$ and τ is increasing to 1, while the left side of Equation 6-8 is 1 at $x_1 = 0$ and decreasing to 0 at $x_1 = \xi = P/K\bar{\rho} < 1$, we must get a single root between 0 and ξ. We find this root by a method of nesting. That is if we set

$$g(x_1, \rho) \equiv (P - K \bar{\rho} x_1) - 4 \rho \tau (P - K x_1)$$

then

$$g(0, \rho) = P > 0$$

$$g(\xi, \rho) = - 4\rho \tau \left(1 - \frac{1}{\bar{\rho}}\right) P < 0 \quad ,$$

since $\bar{\rho} \geq 1$.

This approach allows an initial interval $(0, \xi)$ to be used to bound the root and a new guess is chosen to be $\xi/2$. Then $g(\xi/2, \rho)$ is checked for

its sign and paired with 0 or ξ. One of the previous bounds is discarded and the process repeated. This iteration converged at a slower rate than that for the previous quadratic system where Newton's method was used. When Newton's method was tried for this problem, the iteration became unstable due to large values of e and multiplicity of roots.

A small value of ρ was chosen at the start of the nesting iteration followed by a monotic increase. To obtain a new upper bound for a root $z(\rho)$ for a larger ρ value we may use the root for the previous smaller ρ, since the root $z(\rho)$ as a function of ρ will decrease as ρ increases. That is, if $\rho_1 = \rho + h$ and $z(\rho)$ is the zero for ρ, set $z = z(\rho)$ to get $g[z(\rho), \rho + h] < 0$, since

$$g(z, \rho_1) \equiv g(z) = P - K\bar{\rho}\, z - 2K\, h - 4\rho\, \tau\, (P - Kz) - 4\, h\, \tau\, (P - Kz)$$

$$= - 2K\, h - 4\, h\tau(P - Kz) \ .$$

Since $z < \xi(\rho) < P/K\bar{\rho} < \dfrac{P}{K}$, this is a negative value.

To see that z decreases with ρ increasing, we note that if $g(z, \rho) = 0$.

$$\frac{dz}{d\rho} = - \left(\frac{\partial g}{\partial \rho} \Big/ \frac{\partial g}{\partial z} \right)$$

$$\frac{\partial g}{\partial \rho} = - 2Kz - 4\tau(P - Kz) < 0 \text{ for } 0 < x < P/K$$

$$\frac{\partial g}{\partial z} = - K\bar{\rho} - 4\rho\tau'(P - Kz) + 4\rho\, \tau\, K \quad ,$$

but if z is a root

$$-K(\bar{\rho} - 4\rho\tau) = - K\, \frac{P(\bar{\rho} - 1)}{P - Kz} < 0 \quad .$$

Thus $\frac{dz}{d\rho} < 0$, and the the p_{H_2} is decreasing with increasing ρ.

For values of $0 < \rho < 1/4$, there is only one real positive root and in this case the solutions may be obtained for large e by setting $\tau = 1$. This yields the root

$$z_o = \frac{P}{K} \frac{1 - 4\rho}{1 - 2\rho}$$

which agrees well with computational values. For values of ρ in this range, z_o may be used as a lower bound for the actual root.